

**JHT Final Report**  
**August 1, 2009 – August 31, 2011**

**Improvement in the rapid intensity index by incorporation of inner-core information**

**Principle Investigator:** John Kaplan  
Hurricane Research Division  
NOAA/AOML

**Co-PIs:** Mark DeMaria NOAA/NESDIS, Joe Cione (NOAA/HRD), John Knaff (NOAA/NESDIS), Jason Dunion (CIMAS/HRD), John Dostalek (CIRA), Jun Zhang (CIMAS/HRD)

**Co-Investigators:** Thomas Lee (NRL), Jeffrey Hawkins (NRL), Jeremy Solbrig (NRL)

**Computer and scientist support:** Paul Leighton NOAA/HRD and Evan Kalina (CU)

**Abstract**

In recent years, a statistically based rapid intensification index (RII) that uses predictors from the SHIPS model to estimate the likelihood of RII has been developed for operational use by forecasters at the National Hurricane Center (NHC) for systems in the Atlantic and eastern North Pacific basins. Although the index was found to exhibit some skill when verified for operational forecasts made from 2008-2010, the skill was on the low side underscoring the difficulty of predicting RI.

Thus with support from the NOAA Joint Hurricane Testbed (JHT), research is conducted to try to improve the operational RII by including predictors derived from three new sources of inner-core information. The first of these three new sources is the time evolution of inner-core structure as deduced using standard principle component analysis of GOES infra-red (IR) imagery while the second source is microwave-derived total precipitable water in the near storm environment. The final source is the near storm thermodynamic fields as deduced utilizing GFS temperature and moisture data.

The results of this study indicate that the experimental RII developed using predictors derived from the aforementioned sources is generally more skillful than both climatology and the operational version (save for the 40-kt RI) in both the eastern North Pacific and Atlantic basin when verified for an independent sample of cases from 2008-2010. The finding that the largest improvements in skill (up to 8% in the Atlantic and 5 % in the eastern North Pacific) of the experimental RII over the operational version are observed for the lower RI thresholds may be due, in part, to the relatively small RI sample sizes that are available for the highest RI thresholds. It is interesting to note that an increase in skill with increasing RI threshold magnitude is observed for the eastern North Pacific RII while the opposite trend is observed for the Atlantic basin version. These opposing trends in skill as a function of RI threshold magnitude are also observed for the 2008-2010 operational RII forecasts.

## **1. Operational RII verification**

The current linear discriminant analysis based version of the SHIPS Rapid Intensification Index (RII) has been used operationally at the National Hurricane Center since the start of the 2008 Hurricane season. Figure 1 shows the skill of the operational 2008-2010 RII forecasts for both the Atlantic and eastern North Pacific basins when the RII forecasts were assessed relative to climatology based upon a Brier skill score following the methodology of Kaplan et al. (2010). It can be seen that the RII forecasts were generally skillful (except for the 35-kt threshold in the Atlantic) in each basin. Interestingly, the skill of the RII is found to decrease as the RI threshold increases in the Atlantic basin while a trend of increasing skill with increasing RI threshold magnitude is found for the eastern North Pacific.

Although the aforementioned results indicate that the current operational RII did exhibit some skill for the period 2008-2010, the skill was still on the low side for this period underscoring the need for additional research to improve the RII. Thus, the motivation of this current JHT project has been to attempt to improve the existing operational RII by adding predictors derived from three new sources of information: total precipitable water (TPW) deduced from SSM-I imagery that was archived and processed for the period (1995-2008) by the Naval Research Laboratory (NRL) and the NESDIS operational blended TPW (Kidder and Jones 2007; 2008-2010), principle components derived from analysis of GOES-IR imagery, and boundary-layer predictors deduced from low-level GFS temperature and moisture fields. A description of the newly derived experimental Atlantic and eastern North Pacific versions of the RII that were developed using these new data sources is provided below.

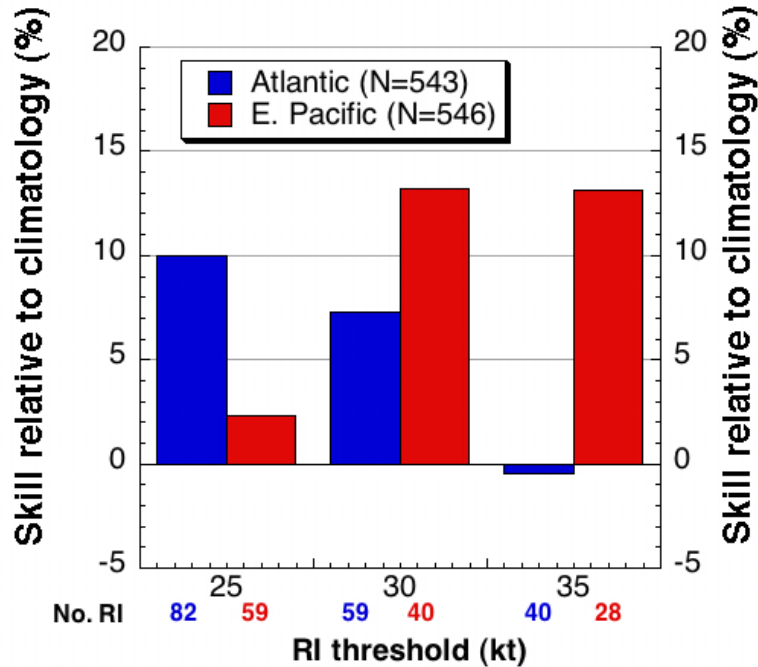


Fig. 1. The skill of the 2008-2010 operational RII forecasts. The number of RI cases for each RI threshold is also provided for both the Atlantic (blue) and eastern North Pacific (red) basins.

## 2. Derivation of Experimental RII

### a. Atlantic Experimental RII

As a first step at screening predictors derived from the above three new sources for their ability to increase the skill of the operational RII, each was subjected to statistical significance testing for a homogenous sample of Atlantic cases for the 1995-2008 sample. Those predictors whose mean values for the developmental RI and non-RI samples were shown to be statistically different (at  $\geq 99.9\%$  level based upon a standard 2-sided t-test) were tested for their ability to increase the skill of the operational RII. This was accomplished by substituting the statistically significant predictors for select predictors in the existing operational RII shown in Table 1. Specifically, the new TPW predictors were tested as replacement to the 850-700 mb relative humidity (RH) predictor since both are measures of atmospheric moisture, while the GOES-IR PC predictors were tested as replacement for the two existing inner-core GOES predictors since they are all measures of inner-core organization as deduced using GOES IR imagery. Finally, the new GFS boundary-layers predictors were tested as a replacement predictor for the potential intensity and ocean heat content predictors, since each of these is related to boundary-layer processes.

Previous 12-h intensity change
850-200 mb vertical shear from 0-500 km radius (24-h mean)
200 mb divergence from 0-1000 km radius (24-h mean)
850-700 mb relative humidity from 200-800 km radius (24-h mean)
% area from 50-200 km covered by $-30^{\circ}\text{C}$ GOES-IR brightness temperatures at T=0 h
Std. dev of 50-200 km GOES-IR brightness temperatures at T= 0 h
Potential intensity (Current intensity – maximum potential intensity)
Oceanic heat content (24-h mean)

Table 1. Predictors used in the current operational Atlantic RII.

Sensitivity tests were then performed to determine if any of the new predictors increased the skill of the RII when they were substituted for the specified predictors described above that are currently included in the existing operational RII (see Table 1). The change in skill of each of the new predictors was then assessed by comparing the average skill of the experimental RII to that obtained using the current operational RII predictors for the three RI thresholds that are used in the current operational RII (25-kt, 30-kt, and 35-kt) as well as an additional RI threshold of 40-kt for which a version of the RII was developed and tested at the request of one of our NHC points of contact (Eric Blake) using the methodology described in Kaplan et al. (2010).

Based upon the above sensitivity tests, three new predictors were selected for use in the new experimental versions of the RII. The first of these predictors is the percentage of the area within 500 km radius  $90^{\circ}$  upshear of the storm center with TPW  $< 45$  mm at time T=0 h. This predictor is used as a replacement to the 850-700 mb RH in the new experimental version of the Atlantic RII. Rapid intensification is favored when this predictor is small and hence the amount of dry air that is being advected into the storm circulation is relatively low. The cutoff of 45 mm as a delineator for dry air is based upon the results of Dunion (2011). Figure 2 shows an example of the distribution of TPW on a select day during the 2003 Hurricane season as well an example of the new blended NESDIS TPW product that is currently used in real-time. Note that the blue and green areas (TPW  $< 45$  mm) represent regions where the atmosphere is relatively dry between the surface and 500 mb (where 90-95% of the contribution from TPW comes from) while the orange and red areas (TPW  $> 45$  mm) represent regions where the atmosphere is relatively moist.

## Total Precipitable Water (TPW) RII Predictor

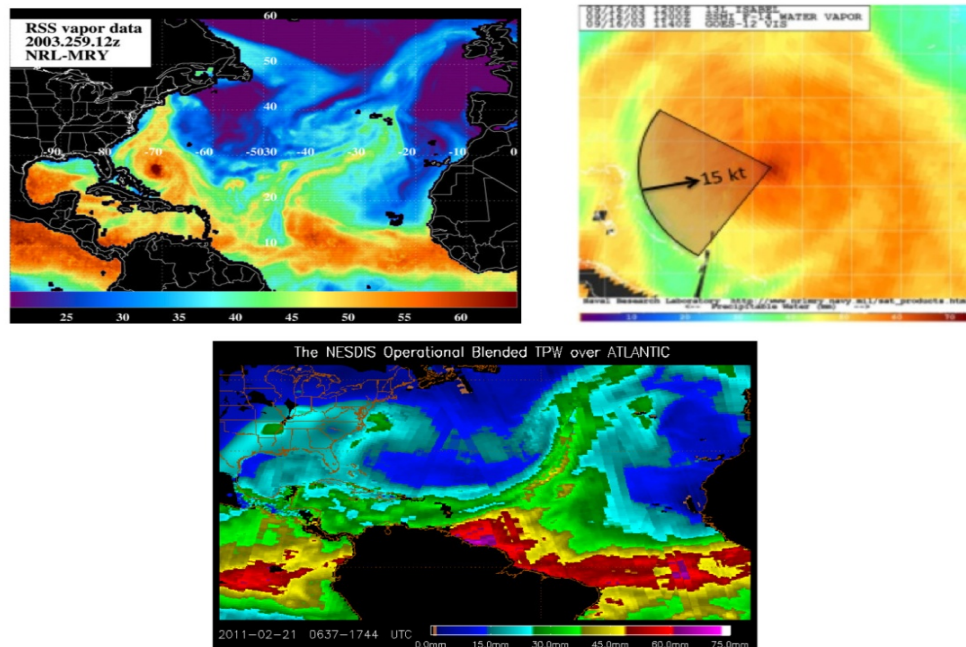


Fig. 2. Total precipitable water (TPW) analysis at 9/16/03 at 12 UTC courtesy NRL (top left panel). A close-up view showing the area over which the TPW predictor is computed is also depicted for Hurricane Isabel located several hundred kilometers east of Florida at this time (top right panel). Finally, an example of the new blended NESDIS operational TPW analysis product that is currently used in real-time is also provided (bottom panel).

The second new RI predictor is the second principle component (PC2) computed from the GOES-IR imagery following the methods described in Knaff (2008). This predictor is used as a replacement for the percent area covered with GOES-IR brightness temperatures  $< -30^{\circ}\text{C}$  in the new experimental version of the Atlantic RII. Figure 3 shows the favored overall pattern of the EOF for PC2 as well as an example of what the GOES-IR imagery looked like just prior to Hurricane Wilma's period of RI during the 2005 Hurricane Season. The image shows that convection tends to be enhanced in the left front quadrant while being suppressed in the right rear quadrant near the time that RI commences. This pattern often precedes axisymmetrization of the IR imagery deduced convection (Knaff 2008). Perhaps, this finding suggests that systems that undergo RI are more likely to be moving into a region where the thermodynamic environment is relatively favorable since such an environment would tend to be more likely to support enhanced convection.

## GOES IR Principle Component (PC) RII Predictor

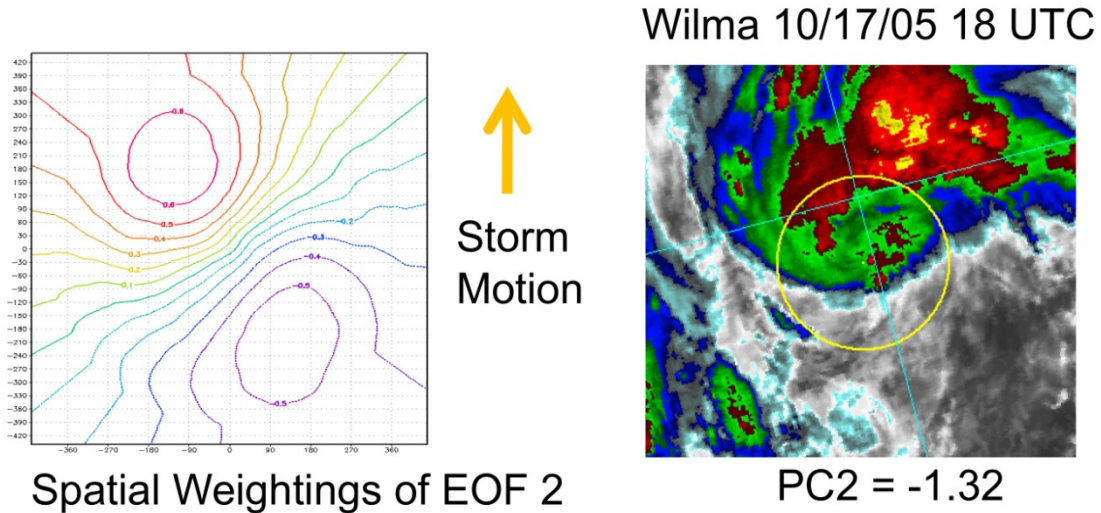


Fig. 3. Preferred pattern of PC2 (left) and an example of the corresponding GOES-IR representation for Hurricane Wilma at 18 UTC on 17 October (right). The yellow circle denotes a circle with a radius of 440 km over which the PCs were evaluated. The direction of motion is to the top center of both diagrams.

The last new predictor is the inner-core dry air predictor that is given by:

$$(q10_{\text{layer}} - q10) * V_{\text{mx}}, \tag{1}$$

where  $q10$  is the inner-core specific humidity at 10 m obtained using the GFS 1000 mb temperature and relative humidity (RH) between 200 and 800 km radius,  $q10_{\text{layer}}$  is the 10 m specific humidity obtained using the ambient 200-800 km radius 1000 mb temperature (T) and the layer-mean RH from 1000 mb to 500 mb, and  $V_{\text{mx}}$  is the NHC maximum sustained wind at  $t=0$  h. The value of  $q10$  is obtained by bringing the 1000 mb air down to the surface (dry adiabatically if unsaturated at 1000 mb and moist adiabatically if air is saturated) and then allowing the air to cool assuming that the RH reaches 95% as the parcel spirals into the storm core (Cione and Uhlhorn 2003). The value of  $q10_{\text{layer}}$  is obtained following the same methodology using the 1000 mb T but using the layer-mean RH between 1000 and 500 mb instead of using only the RH at 1000 mb. It should be noted that small values of the inner-core dry air predictor, indicating less potential for dry air to mix down to the surface, are favored for RI. Although initial testing of this predictor as a replacement for potential intensity and/or ocean heat content on cases from the 1995-2008 database showed that it increased the skill of the RII when used in place of ocean heat content, additional testing conducted after cases from the 2009 Hurricane Season were added to the existing database showed that the skill of the RII was maximized when all three (ocean heat content, inner-core dry air predictor, and

potential intensity) were used as RII predictors. Thus, the new experimental version of the Atlantic RII has a total of 9 predictors as is shown in Table 2.

Finally, in addition to utilizing three new RI predictors, the scaling methodology that was used for the potential intensity and persistence predictors was modified slightly since sensitivity tests showed that doing so improved the overall skill of the model for the developmental sample. This new scaling technique was formulated so that the both the potential and persistence values were most favored for RI when they were equal to the mean value of each respective RI predictor for all of the RI cases in the developmental sample. Figure 4 shows that this new experimental RII yielded an increase in skill of anywhere from 2 – 6 % over the current operational version for the developmental sample with an average absolute skill improvement of 3 % (15% relative improvement) observed for the four RI thresholds studied.

Previous 12-h intensity change
850-200 mb vertical shear from 0-500 km radius (24-h mean)
200 mb divergence from 0-1000 km radius (24-h mean)
Percent area with TPW < 45 mm within 500 km radius 90° upshear (T= 0 h value)
Second principle component of GOES-IR imagery within 440 km radius (T=0 h value)
Std. dev of 50-200 km GOES-IR brightness temperatures (T= 0 h value)
Potential intensity (Current intensity – maximum potential intensity)
Oceanic heat content (24-h mean)
Inner-core dry air predictor (24-h mean)

Table 2. Predictors used in the new experimental Atlantic RII.

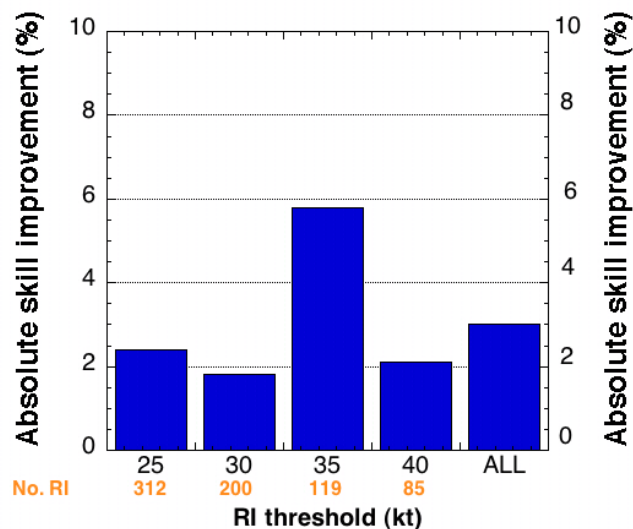


Fig. 4. Improvement of the new Atlantic Experimental RII over the current operational version for the 1995-2009 dependent sample (N=2524). The number of RI cases for each RI threshold are shown in orange along the x-axis.

b. Eastern North Pacific Experimental RII

An eastern North Pacific version of the RII index that included the same nine predictors that were used in the Atlantic experimental RII described above as well as one additional predictor (the initial NHC estimated maximum sustained wind) was derived using data for the period 1995-2009. A list of the predictors used in the new experimental eastern North Pacific RII is provided in Table 3. It should be noted that the new scaling methodology that was originally developed for use in the experimental version of the Atlantic RII degraded the eastern North Pacific version when tested on the developmental sample. Thus, when deriving the new experimental version of the eastern North Pacific RII, the persistence and potential predictors were treated using the same methodology that is used in the current operational RII. The results depicted in Fig. 5 indicate that the new experimental eastern North Pacific RII exhibited mean absolute improvements ranging from 0.2-3.2% with an average absolute skill improvement of 2 % (10% relative improvement) over the current operational version for the four RI thresholds for the dependent sample studied.

Previous 12-h intensity change
850-200 mb vertical shear from 0-500 km radius (24-h mean)
200 mb divergence from 0-1000 km radius (24-h mean)
Percent area with TPW < 45 mm within 500 km radius 90° up-shear at T=0 h
Second principle component of GOES-IR imagery within 440 km radius at T= 0 h
Std. dev of 50-200 km GOES-IR brightness temperatures at T= 0 h
Potential intensity (Current intensity – maximum potential intensity)
Oceanic heat content (24-h mean)
Inner-core dry air predictor (24-h mean)
T=0 h maximum sustained wind

Table 3. Predictors used in the new experimental E. Pacific RII.

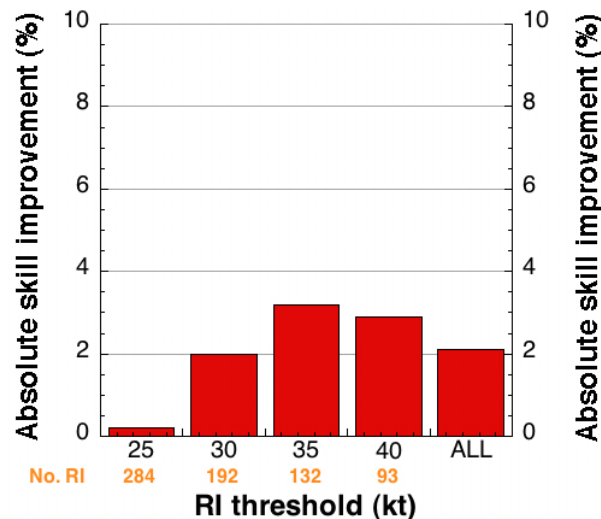


Fig. 5. Improvement of the new eastern North Pacific Experimental RII over the current operational version for the 1995-2009 dependent sample (N=2422). The number of RI cases for each RI threshold is depicted in orange along the x-axis.

### 3. Results

#### a. Atlantic Experimental RII Verification

Since the experimental version of the Atlantic RII was only first run in real-time and made available to forecasters at the NHC via a web site at CIRA in mid September of the 2010 Hurricane, it was re-run for all cases from 2008-2010 to provide a more representative assessment of its likely level of performance when run in an operational environment. To accomplish this all of the forecast cases from 2008-2010 were re-run using the real-time GFS forecast fields and the NHC forecast tracks. Prior to performing the re-runs for a given year, both the operational and experimental versions of the RII were first re-derived by excluding all cases from that particular year. Consequently, the skill shown below should closely mimic that which would have otherwise been obtained had these forecasts been made in real-time for this three-year period. It should be noted that the number of re-run forecasts is slightly lower than the number of operational forecasts since the data required to compute the PC predictor were not available for some forecasts made early in a storm's lifecycle, particularly for cases prior to 2010 when this predictor was not routinely computed.

Figure 6 shows the skill of the Atlantic RII for the original experimental version of the RII (Experimental\_V1) as well as for a second version of the RII that was derived using the same predictors (see Table 3) and methods that were used to derive the eastern North Pacific version described above. This second version (Experimental\_V2) was tested since it is desirable to have the same version of a model running in both basins and dependent tests showed that it was also superior to the version that had been previously developed for use in the Atlantic. It is worth noting that these results are basically an update of those contained the mid-term report except that the Experimental\_V2 results have been modified since it was recently discovered that some of the input files that were used to obtain the previously reported results were erroneous.

Inspection of the figure reveals that the new Experimental\_V2 version of the Atlantic Experimental RII was more skillful than the previously developed Experimental\_V1 version for all 4 RI thresholds. It is also noteworthy that the new Experimental\_V2 version performed best relative to the operational version at the lower RI thresholds with the largest absolute skill improvement of 8 % (which represents over a 200% relative skill improvement) being observed for the 30-kt RI threshold. Perhaps, the relatively small RI sample sizes at the higher RI thresholds are responsible for the less impressive performance of the Experimental Atlantic RII for those thresholds. Alternatively, perhaps the degradation in performance is due to a greater sensitivity to the use of real-time GFS forecast fields and NHC forecast tracks for the re-run forecasts made for the higher RI thresholds.

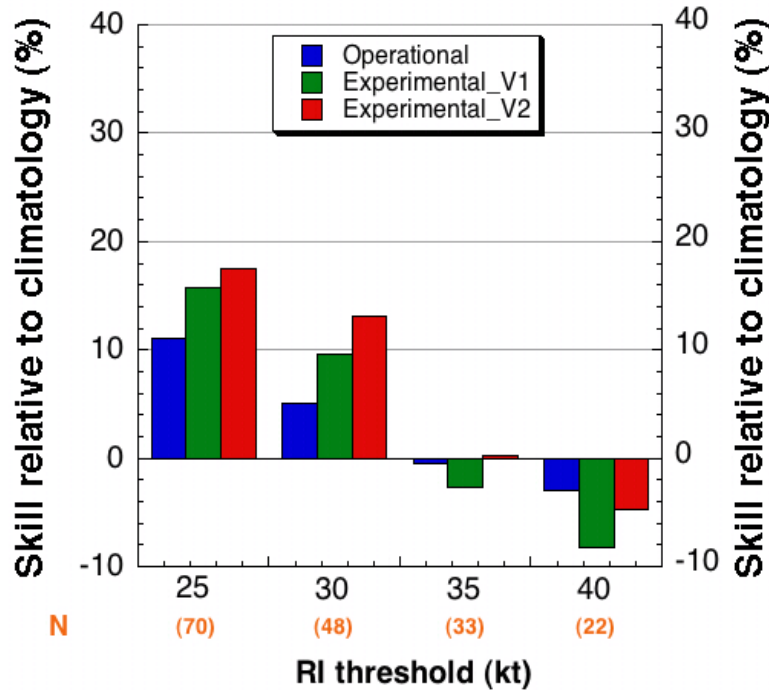


Fig. 6. Skill of the new Experimental Atlantic RII for both the original (Experimental\_V1) and the newest (Experimental\_V2) formulation for the 2008-2010 independent re-run forecasts (N=503). Also shown for comparison is the skill of the operational version of the RII for those same forecasts. The number of RI cases for each RI threshold is provided in orange.

#### b. Eastern North Pacific Experimental RII Verification

Figure 7 shows the skill of the eastern North Pacific 2008-2010 re-run forecasts that was obtained using the same verification methods that were used for the Atlantic basin. It can be seen that the new experimental eastern North Pacific RII was generally more skillful than the current operational version for the lowest three RI thresholds (25-kt, 30-kt, and 35-kt) by anywhere from 0.7 to 5.2 % (which represents a 15-40% relative skill improvement) but had less skill for the 40-kt RI threshold although both versions were still quite skillful for this threshold. It is hypothesized that the finding of lower skill for the Experimental RII at the 40-kt RI threshold is due, in part, to the relatively small number of RI cases that were available both to develop and verify the RII forecasts that were made for this threshold. For this reason, it is hypothesized that when additional RI cases are added improvements similar to those that were obtained for the developmental sample (Fig. 5) can be achieved. It is interesting to note that in addition to exhibiting more skill than the Atlantic versions of the RII, both the experimental and operational versions of the eastern North Pacific RII exhibited increasing skill with increasing RI threshold magnitude while Fig. 6 shows that the new Experimental versions of the Atlantic RII showed the opposite trend of decreasing skill with increasing RI threshold magnitude. These opposing trends in skill as a function of RI threshold magnitude for the Atlantic and eastern North Pacific basins were also found for the 2008-2010 operational RII forecasts (Fig. 1).

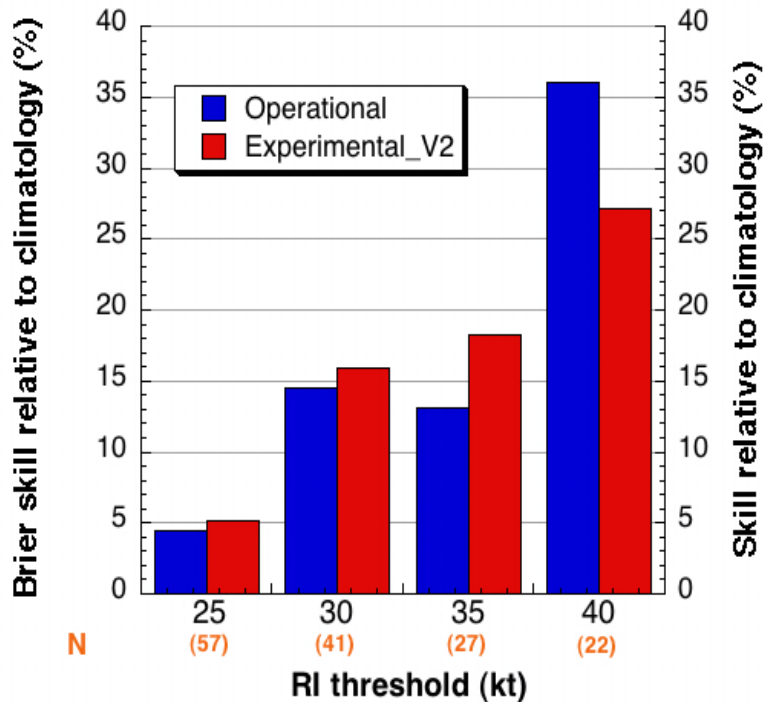


Fig. 7. Skill of the operational and experimental\_V2 version of the eastern North Pacific RII for the independent 2008-2010 re-run forecasts (N=509). Also shown for comparison is the skill of the operational version of the RII for those same forecasts. The number of RI cases for each RI threshold is also shown in orange.

#### 4. Preparation of Experimental RII for real-time use for 2011 Hurricane Season

In preparation for testing during the 2011 Hurricane Season, revised versions of the new experimental Atlantic and eastern North Pacific RII were derived using the updated SHIPS database that included cases from the 2010 Hurricane Season. These new routines were then installed on a server at CIRA in Fort Collins, CO and were run in near-real time (within about ½ an hour of the operational version) commencing on 1 August 2011. The output of these real-time runs as well as re-runs that were done for systems that occurred prior to August 1 are currently being made available to NHC forecasters via a real-time link at CIRA.

Figure 8 shows an example of the performance of the new experimental version of the RII as well as the operational version for Hurricane Adrian (2011). Although the experimental RII results were not available in real-time they were obtained using the 2011 version of the experimental RII and the same real-time analysis and forecast field data that were used by the operational version. The figure indicates that although both versions showed high RI probabilities at the time when RI first commenced, the experimental version correctly showed continuously high probabilities of RI during the entire period during which RI was observed while the operational RII probabilities decreased too quickly. Inspection of the individual RI forecasts indicates that the rapid decrease in RII probabilities of the operational version of the RII was due to the values of the relative humidity RI predictor falling outside the range of values for which RI had

been previously been observed which resulted in very low RI probabilities being assigned.

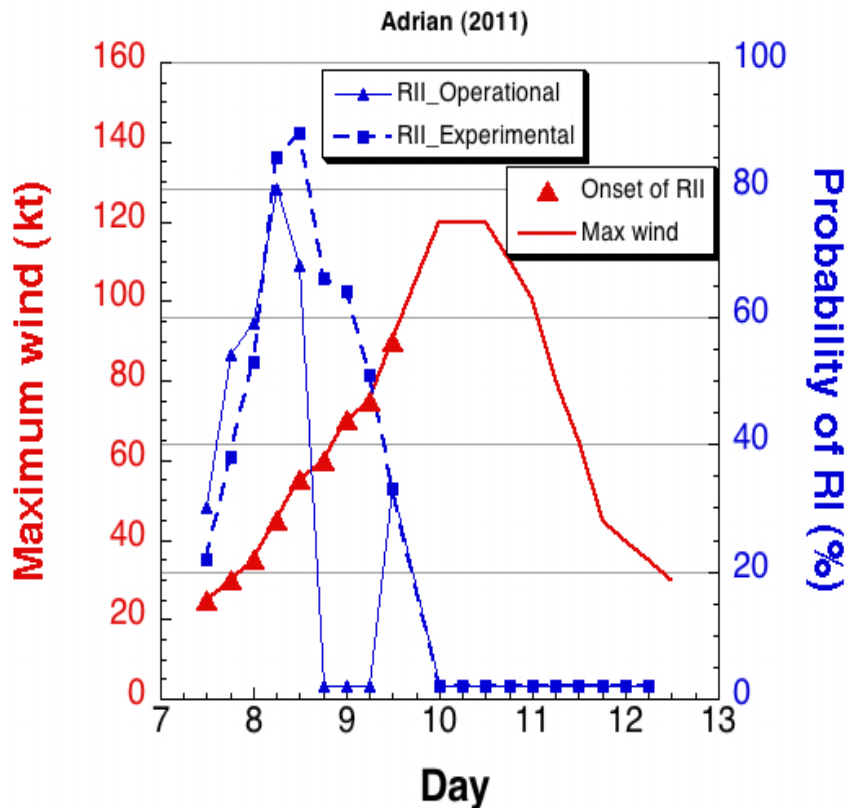


Fig 8. The probability of RI for the operational (solid blue) and new experimental (dashed blue) versions of the RII for eastern North Pacific Hurricane Adrian (2011). The NHC real-time maximum sustained wind estimates (solid red line) and the initial (T=0 h) times at which RI commenced (red triangles) are also provided.

### 5. Transition of code for computing TPW and PC predictor in real time

The code to calculate TPW and IR PC predictors for the experimental version of RII has been tested at CIRA the last two hurricane seasons. While the TPW can continue to be processed in the same manner, but on a JHT server, the code that calculates the IR PCs will need to be transitioned to the NCEP IBM and make use of the IR data flow on that machine.

The TPW predictors are created from the NESDIS operational blended TPW product (Kidder and Jones 2007) that is distributed in HDF format by an operational ftp server at NESDIS. A python script mirrors these data on a local server and FORTRAN 90 code converts the HDF into two gridded files covering the Atlantic and eastern North Pacific tropical storm basins. This code has already been installed on the JHT servers at NHC where it has been creating the ascii files since May 2011. To create the predictors these ascii files would have to be pushed to the NCEP IBM where they can be accessed by the SHIPS/LGEM/RII model processing scripts. Code already exists to calculate the

TPW predictors from information in the large-scale diagnostic files (\*.lsdiag), which can be added to the SHIPS/LGEM/RII scripts.

Unlike the TPW predictors, IR predictors require access to the GOES IR imagery, which is currently available to the RII on the NCEP IBM (though other data ingests could be developed). Presuming that this method to access the IR data continues, Fortran code that 1) creates storm direction relative analyses 2) calculates the IR PCs and 3) constructs the time averaged IR PC used for this project would have to be modified to work with the IBM IR imagery data flow. These programs are currently running at CIRA, but are fed by a real-time data feed associated with the CIRA TC IR image archive, which consists of 4km Mercator IR images from GOES channel 4 and MSG channel 9 imagery. The modular nature of the code should make the implementation of these routines on the NCEP IBM relatively routine.

#### References:

Cione, J.J., and E.W. Uhlhorn, 2003: Sea Surface temperature variability in hurricanes: Implications with respect to intensity change. *Mon. Wea. Rev.*, **131**, 1783-1796.

Dunion, J.D., 2011: Rewriting the climatology of the tropical North Atlantic and Caribbean Sea atmosphere. *J. Climate*, **24**, 893-908.

Kaplan, J., M. DeMaria and J. A. Knaff, 2010: A revised tropical cyclone rapid intensification index for the Atlantic and eastern North Pacific basins. *Wea. Forecasting*, **25**, 220-241.

Kidder, S. Q., A. S. Jones, 2007: A blended satellite total precipitable water product for operational forecasting. *J. Atmos. Oceanic Technol.*, **24**, 74-81.

Knaff, J.A., 2008: Rapid tropical cyclone transitions to major hurricane intensity: Structural evolution of infrared imagery. *Preprints 28<sup>th</sup> Conf. on Hurricanes and Tropical Meteorology*, Orlando, FL, Amer. Meteor. Soc. .